Supporting Information

# Benzothiazole-Based Covalent Organic Frameworks with Different Symmetrical Combinations for Photocatalytic $CO_2$ Conversion

*Young Hyun Kim*[§, †], *Nayeong Kim*[§, ‡], *Jeong-Min Seo*[†], *Jong-Pil Jeon*[†], *Hyuk-Jun Noh*[†], *Do Hyung Kweon*[†], *Jungki Ryu*[‡*], *Jong-Beom Baek*[†*]

†School of Energy and Chemical Engineering/Center for Dimension-Controllable Organic Frameworks, Ulsan National Institute of Science and Technology (UNIST), 50 UNIST, Ulsan 44919, Republic of Korea

‡ Department of Energy Engineering, School of Energy and Chemical Engineering, and Emergent Hydrogen Technology R&D Center, Ulsan National Institute of Science and Technology (UNIST), Ulsan 44919, Republic of Korea

## Table of contents

## S1. Materials and methods

2,4,6-trithiocyanatobenzene-1,3,5-triamine (TCBT), benzo[1,2-d:4,5-d']bis(thiazole)-2,6-diamine (BTzA), 1,3,5-triformylphloroglucinol (Tp) were prepared using the following reported procedure.[1,2,3] Commercially available solvents and reagents were purchased from Sigma-Aldrich, TCI chemicals, Alfa-Aesar and Samchun chemistry. All purchased materials were used without further purification unless stated otherwise.

**Nuclear magnetic resonance (NMR) spectra** were recorded on a Bruker AVANCE III HD spectrometer in the given solvents. Data from the $^{1}$H NMR spectra are reported in the following way: chemical shift (δ) in ppm (multiplicity, integration, assignment). Multiplicities are reported as follows: br = broadened singlet, s = singlet, d = doublet, m = multiplet). Solid state cross polarization magic-angle spinning nuclear magnetic resonance ($^{13}$C CP-MAS NMR) spectra were measured with an Agilent VNMRS 600 spectrometer using 2.5 mm diameter $ZrO_2$ rotors at a spinning frequency of 20 kHz.

**Fourier-transform infrared spectra (FT-IR)** were recorded on a PerkinElmer Spectrum 100 in transmission by pelletizing a sample with KBr.

**Thermogravimetric analysis (TGA) measurements** were conducted on a STA 8000 (PerkinElmer). All samples were heated from room temperature to 900 °C under air and nitrogen atmosphere at a heating rate of 10 °C min$^{-1}$.

**Powder X-ray diffraction data (PXRD)** were collected using a Rigaku D/Max 2500 rotating anode X-ray powder diffractometer using Cu Kα radiation (λ = 1.5406 Å) operated at 1.6 kW (40 kV, 40 mA) power and equipped with a position sensitive detector with a 10.0 mm divergence height slit. Samples were loaded on zero background sample holders. Data were collected in the range of $2\theta$ = 2 to 50° with a 0.02° of step size and 1° min$^{-1}$ of scan rate. Pawley refinement was performed to optimize the lattice parameter repeatedly. The Pseudo-Voigt function was used for whole profile fitting, and the Berar-Baldinozzi function was used for asymmetry correction during the refinement processes until the $R_p$ and $wR_p$ values converged.

**Chemical stability testing** was carried out by immersing the COF powder into an acid/base solution for 3 days. All samples were collected by filtration and retained crystallinity was confirmed by PXRD measurement.

**Field emission scanning electron microscopy (SEM)** was carried out on a FEI Nanonova 230, equipped with an energy dispersive spectrometer, with an accelerating voltage of 10 kV and a working distance of 5 mm. All samples were loaded on the conductive carbon tape and then prepared by Pt sputtering.

**High-resolution transmission electron microscopy (HR-TEM)** was performed with a JEOL JEM-2100F equipped with a field emission gun operated at 200 kV. The sample was suspended in Isopropyl alcohol and drop-cast onto a 200 copper mesh, lacey carbon grid (Ted Pella).

**Elemental analysis (EA)** was conducted on a Thermo Scientific Flash 2000.

**The low-pressure nitrogen adsorption-desorption isotherms** were recorded on a BELSORP-max at 77 K in a pressure range from $P/P_0 = 10^{-6}$ to 0.99. Prior to measurement of the sorption isotherm the samples were degassed for 24 h at 150 °C under high vacuum. To evaluate surface area the Brunauer-Emmett-Teller (BET) model was applied. The calculations of the pore size distribution were performed using the nonlocal density functional theory (NLDFT) adsorption model with an oxygen kernel for cylindrical pores.

**The low-pressure carbon dioxide adsorption-desorption isotherms** were recorded on a BELSORP-max at 298 K and 273K respectively in a pressure range from $P/P_0 = 10^{-6}$ to 0.99. Prior to measurement of the sorption isotherm, the samples were degassed for 24 h at 150 °C under high vacuum.

**UV-visible absorption spectra** were recorded on a Cary 5000 spectrometer equipped with D2 lamp. Absorption spectra were calculated by reflectance data using the Kubelka-Munk function.

**Photoluminescence (PL) spectra** were recorded on a Cray Eclipse spectrometer equipped with Xe lamp and photomultiplier tube detector.

**Time-correlated single photon counting (TCSPC)** were measured on FluoTime 300, equipped with 450-nm continuous wave and pulsed diode laser head (LDH-D-C-450) coupled with a laser diode driver (PDL 820). Each decay curve was fitted using the associated fitting software (FluoFit) to calculate the time constant corresponding to the curves.

**Photoelectrochemical measurement**

For the electrochemical measurement, 0.1 wt% of COF solution was dispersed using an ultrasonicator for 30 min to make a homogenous state. Fluoride-tin oxide (FTO) glass was covered with copper masking tape, giving an area of 1 $cm^2$. The prepared homogenous solution was coated on FTO glass using the spray method and dried overnight at 70 $^oC$ in a vacuum oven. Photocurrent and Nyquist plots were carried out with a SP-150 (Bio-Logic Science Instruments, France) under the following three-electrode configuration: a working electrode, COFs film on FTO; a reference electrode, Ag/AgCl; a counter electrode, fluorine-doped tin oxide coated with 100-nm thick Pt; electrolyte, 0.1 M $KHCO_3$ saturated with $CO_2$ gas (pH 7.0); applied bias potential, -0.4 V versus RHE; and scan rate, 10 mV $s^{-1}$. A 300 W Xe lamp equipped with a 400 nm cut-on filter (100 mW $cm^{-2}$) was used as a light source. For the Nyquist plots, the frequency range was from 0.1 Hz to 100 kHz. Numerical fitting of the Nyquist plots was conducted using EC-lab software (Bio-Logic Science Instruments, France).

**Apparent quantum yield (AQY) for CO production**

The apparent quantum yield of CO production was calculated based on the production yield with different monochromatic LED light. The reaction condition was the same as in the photocatalytic CO2 conversion system and only the light source was changed for the specific wavelength. The AQY was calculated as follows: $AQY\ (\%) = 2 \times [n\ CO \times N_A \times \times \hbar \times c)] \times 100\% / (I \times S \times t \times \lambda)$

where, $N_A$ is the Avogadro constant ($6.022 \times 10^{23}$ $mol^{-1}$), ħ is the Planck constant ($6.626 \times 10^{-34}$ J s), c is the speed of light ($3 \times 10^8$ m $s^{-1}$), S is the irradiation area ($cm^2$), I is the intensity of irradiation light (W $cm^{-2}$), t is the photoreaction time (s), λ is the wavelength of the monochromatic light (m).

## S2. Synthetic procedure

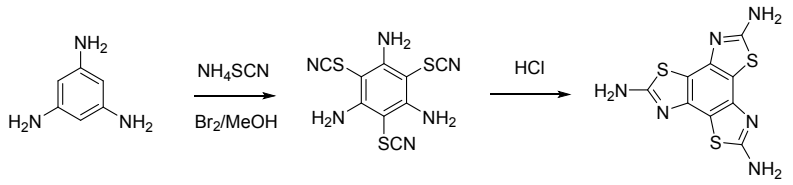


**2,4,6-Trithiocyanatobenzene-1,3,5-triamine**

The synthetic scheme was modified following the literature. A 500 mL round bottom flask was charged with 1,3,5-triaminobenzene (1 g, 8.11 mmol), ammonium thiocyanate (3.71 g, 48.7 mmol) with 10 mL of methanol. Bromine (1.3 mL) was added. The reaction mixture was stirred vigorously for 2 h under room temperature. A saturated potassium bicarbonate ($K_2CO_3$) solution was slowly added into the reaction mixture to remove unreacted bromine. An off-white colored product was collected by filtration and washed with methanol and used directly in the next step without further purification. (Yield = 78%)

**Benzo[1,2-d:3,4-d':5,6-d'']tris(thiazole)-2,5,8-triamine**

A 250 mL round bottom flask was charged with 2,4,6-thiocanatobenzene-1,3,5-triamine and hydrochloride solution. The reaction mixture was stirred for 1 h at room temperature. The resulting product was poured into ice and then collected by filtration. (Yield=85%) $^1$H NMR (400 MHz, DMSO-$d_6$) δ 7.53 (s, 2H, *$NH_2$*); $^{13}$C NMR (100 MHz, DMSO-$d_6$) δ 166.71, 143.52, 119.09.

**Synthesis of TTzTp** benzo[1,2-d:3,4-d':5,6-d'']tris(thiazole)-2,5,8-triamine (TTz, 0.084 g, 0.286 mmol), 1,3,5-triformylphloroglucinol (Tp, 0.060 g, 0.286 mmol), N-methyl-2-pyrrolidone (NMP, 2.4 mL), 1,3,5-trimethylbenzene (Mesitylene, 2.4 mL) and 6 M acetic acid (0.48 mL) were filled into a 50 mL glass ampoule. The reaction mixture was sonicated for 30 min to obtain a homogeneous dispersion and then degassed three times by free-vacuum thaw cycles, flash frozen at 77 K (liquid $N_2$ bath) evacuated to an internal pressure below 100 mTorr and flame sealed. The reaction mixture was kept undisturbed at 120 °C for 72 h. The product was collected by filtration and washed with acetone, methanol and N-methyl-2-pyrrolidone. The collected red colored powder was freeze dried to prevent shrinkage.

**Synthesis of BTzTp** benzo[1,2-d:4,5-d']bis(thiazole)-2,6-diamine (BTz, 0.09 g, 0.404 mmol), 1,3,5-triformylphloroglucinol (Tp, 0.056 g, 0.269 mmol), N-methyl-2-pyrrolidone (NMP, 2.4 mL), 1,3,5-

trimethylbenzene (Mestiylene, 2.4 mL) and 6 M acetic acid (0.48 mL) were charged into a 50 mL glass ampoule. The subsequent process was the same as that for TTzTp.

## S3. Powder X-ray diffraction analysis

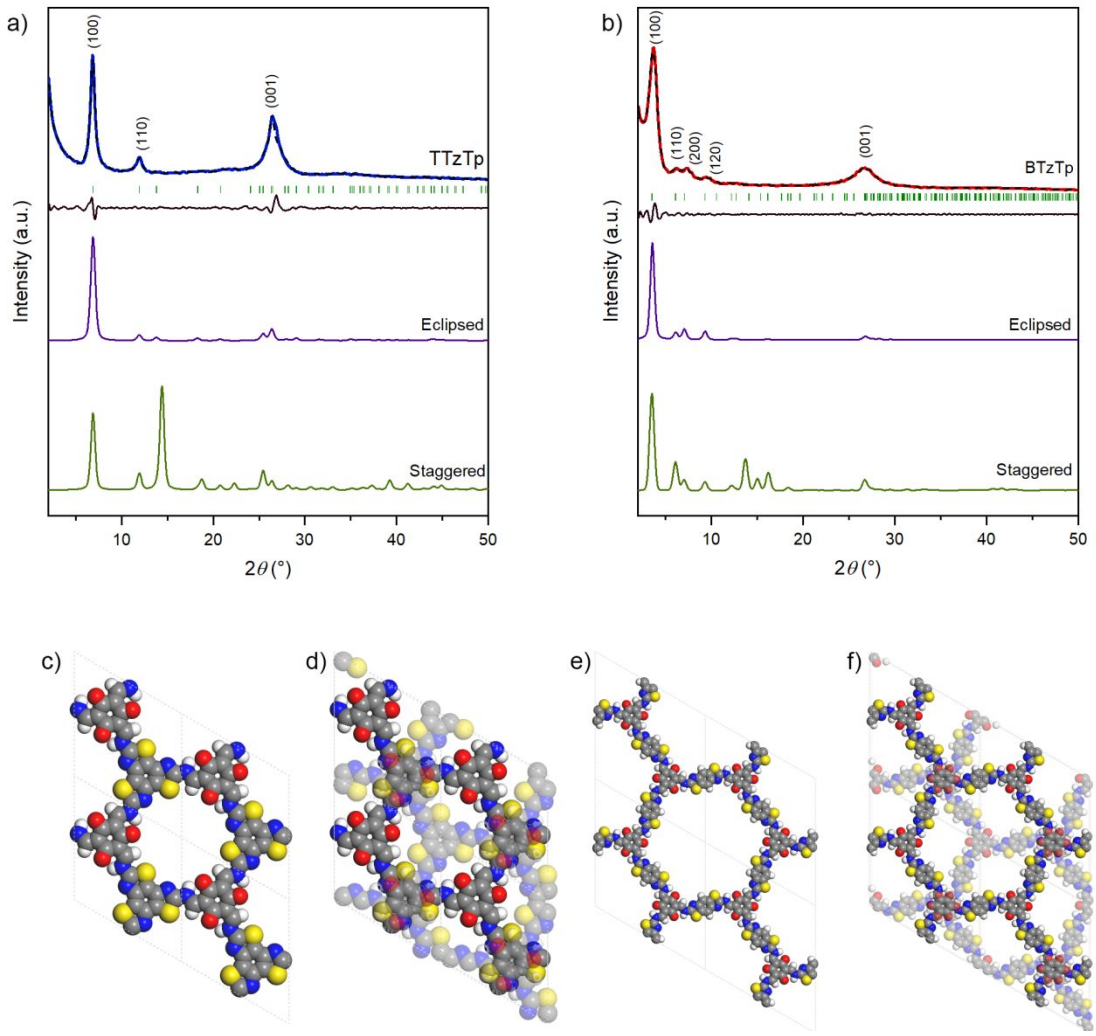


**Figure S1.** PXRD patterns of TTzTp and BTzTp. (a) Experimental (red line), Pawley-refined pattern (black-dashed line), Bragg position and difference plot (cyan), simulated results of TTzTp with eclipsed and staggered model. (b) Experimental (light brown line), Pawley-refined pattern (black-dashed line), Bragg position and difference plot (cyan), simulated results of BTzTp with eclipsed and staggered model. Crystallographic unit cell of TTzTp with (c) eclipsed (a=b=14.815 Å, c=3.5 Å , space group *P3*) and (d) staggered (a=b=29.646 Å, c=7.2 Å space group *P1*) (d) and BTzTp with (e) eclipsed (a=b=29.050 Å, c=3.34 Å space group *P6/M*) and (f) staggered (a=b=29.050 Å, c=6.68 space group *P63/M*)

**Table S1. Calculated value of FWHM and maximum intensity ratio of maximum intensity for (100) and (001) reflection of XRD results**

| Entry | FWHM | Intensity ratio ($I_{(100)}/I_{(001)}$) |
|---|---|---|
| TTzTp | 0.496 | 2.03 |
| BTzTp | 0.899 | 5.68 |

## S4. HR-TEM images

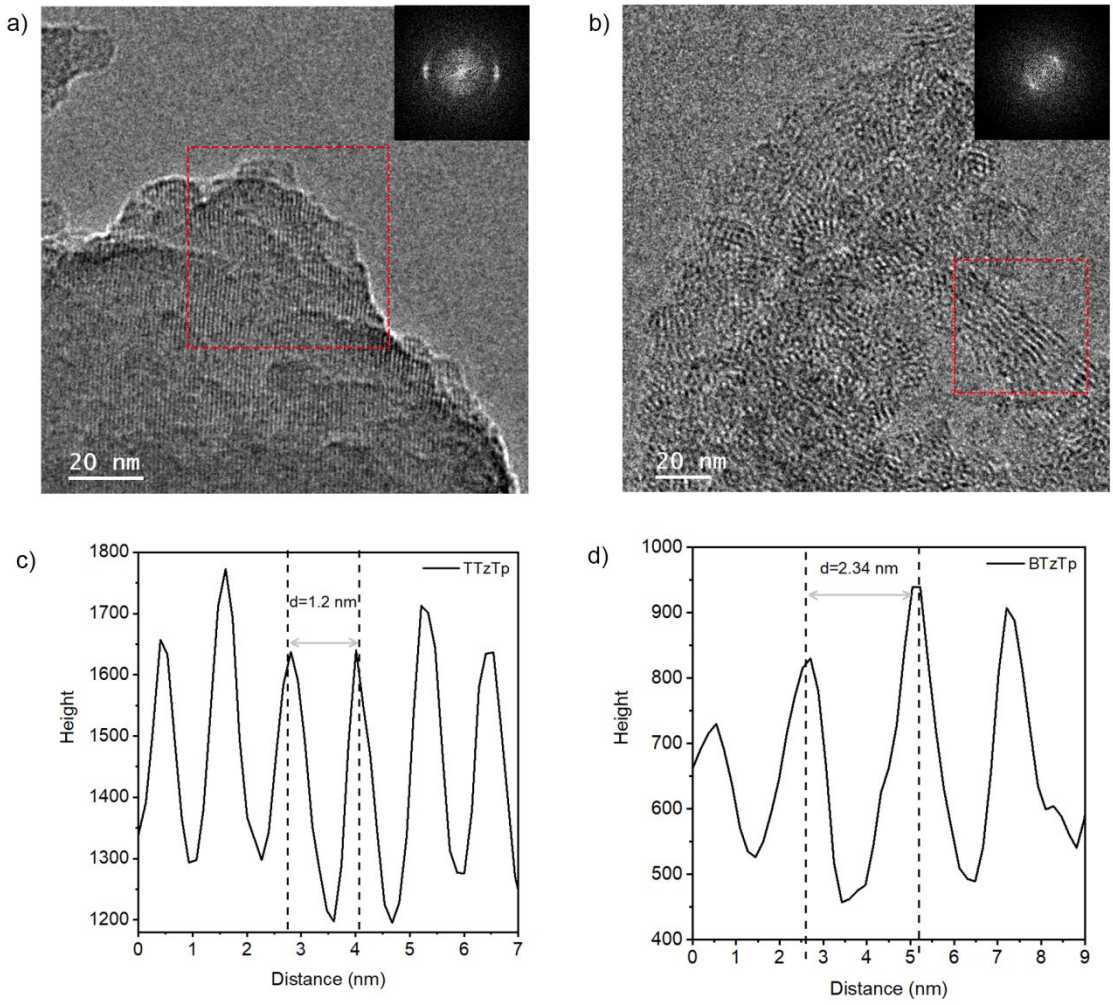


**Figure S2.** HR-TEM images of (a) TTzTp and (b) BTzTp showing their crystalline morphology, and *d*-spacing indexes of (c) TTzTp and (d) BTzTp.

## S5. FT-IR spectroscopy comparision

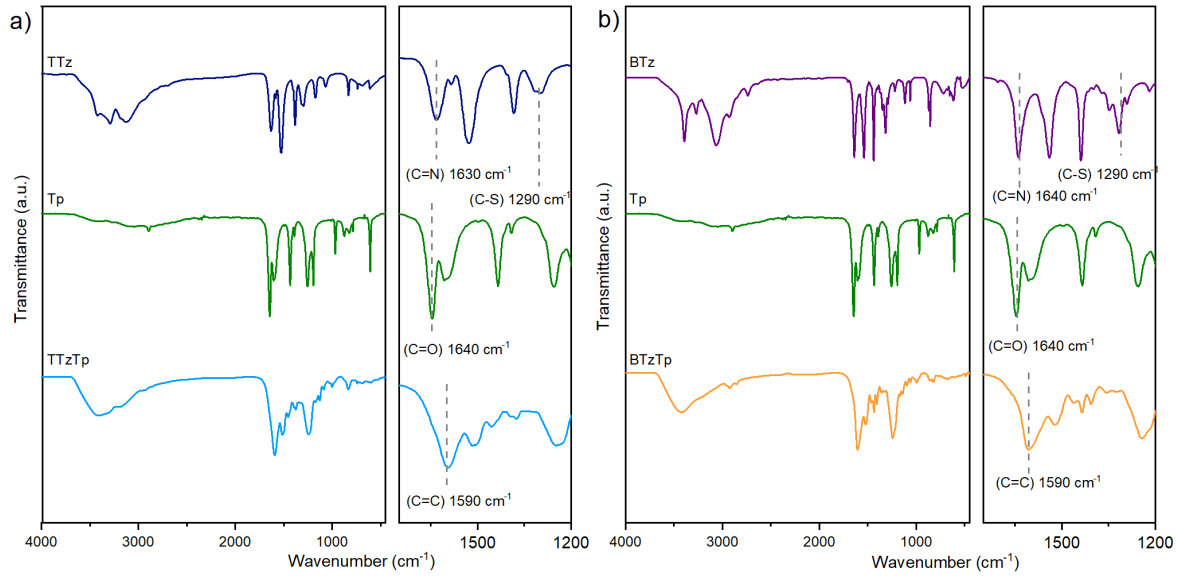


**Figure S3.** FT-IR spectroscopy of (a) TTz (navy), Tp (green) and TTzTp (blue) (b) BTz (purple), Tp (green) and BTzTp (orange).

## S6. Thermal and chemical stability

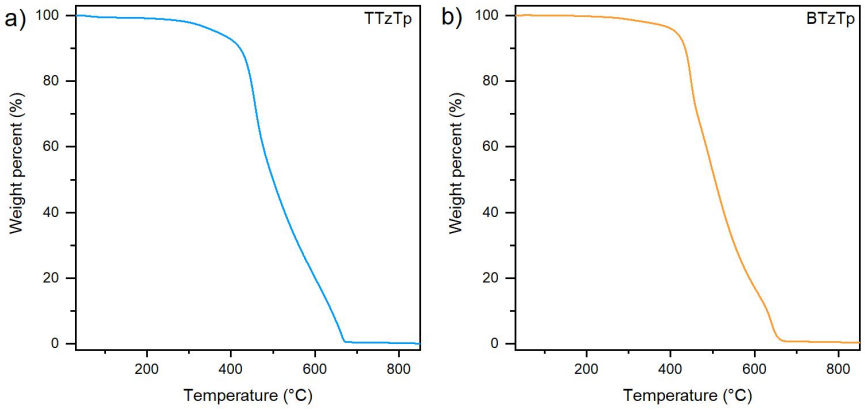


**Figure S4**. TGA curve of (a) TTzTp (blue) and (b) BTzTp (orange).

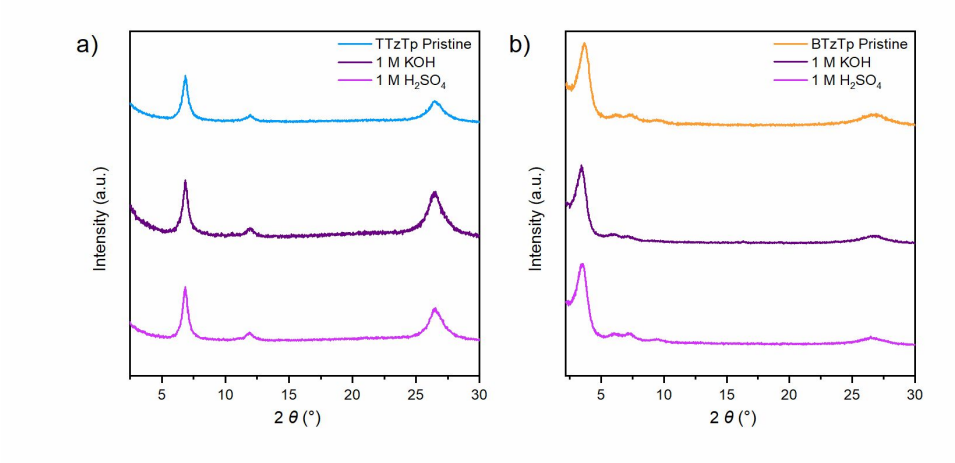


**Figure S5**. PXRD after chemical stability testing with different acid and base conditions (a) TTzTp and (b) BTzTp.

## S7. UV-vis spectra and cyclic voltametry

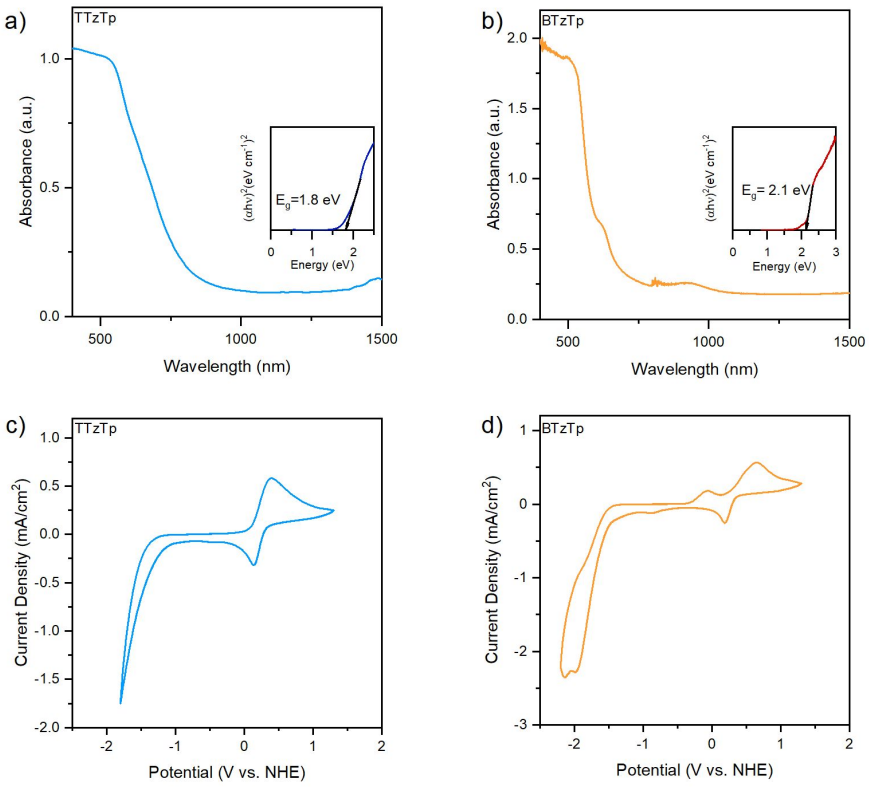


**Figure S6.** UV-vis diffuse reflectance spectra (DRS) with an inset tauc plot for the optical bandgap of TTzTp (a) and BTzTp (b) and cyclic voltammetry (CV) for TTzTp (c) and BTzTp (d).

**Table S2.** The fitting results for EIS spectra of TTzTp and BTzTp

| | $R_s$ (Ω) | $R_1$ (Ω) | $CPE_1$ (F) |
|---|---|---|---|
| TTzTp | 90.44 | 20610 | $21.67\times10^{-6}$ |
| BTzTp | 63.02 | 10500 | $14.16\times10^{-6}$ |

## S8. Photocatalytic $CO_2$ conversion experiment

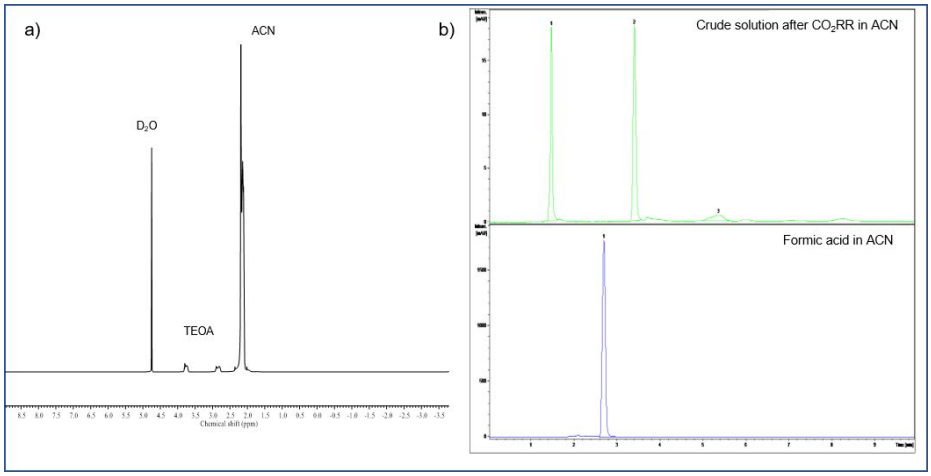


**Figure S7.** NMR spectra and high-resolution liquid chromatography (HPLC) analyses of the crude solution after the photocatalytic $CO_2$ reduction reaction.

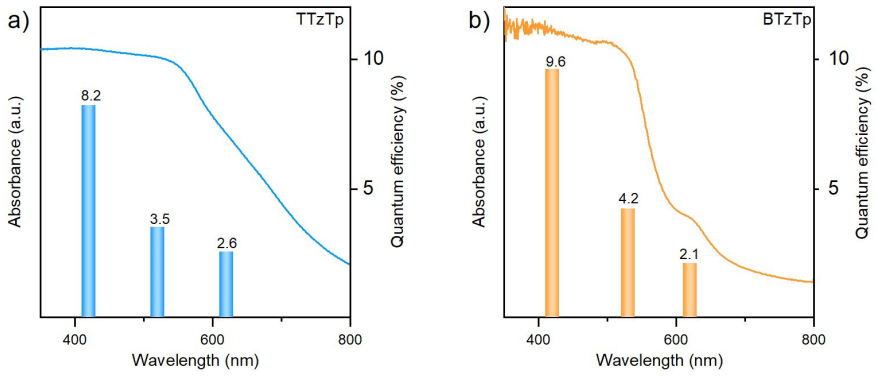


**Figure S8.** UV-vis diffuse reflectance spectra (DRS) with apparent quantum efficiency (AQE) for (a) TTzTp and (b) BTzTp.

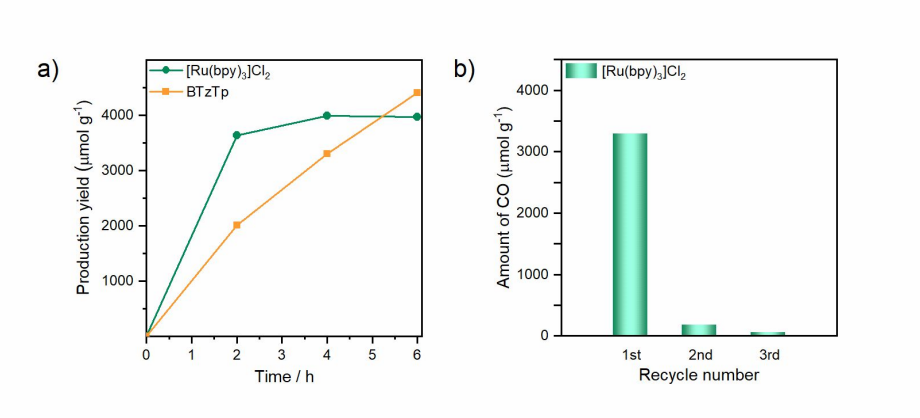


**Figure S9.** Photocatalytic $CO_2$ to CO conversion of $[Ru(bpy)_3]Cl_2$ and BTzTp after 6 h, and recyclability test.

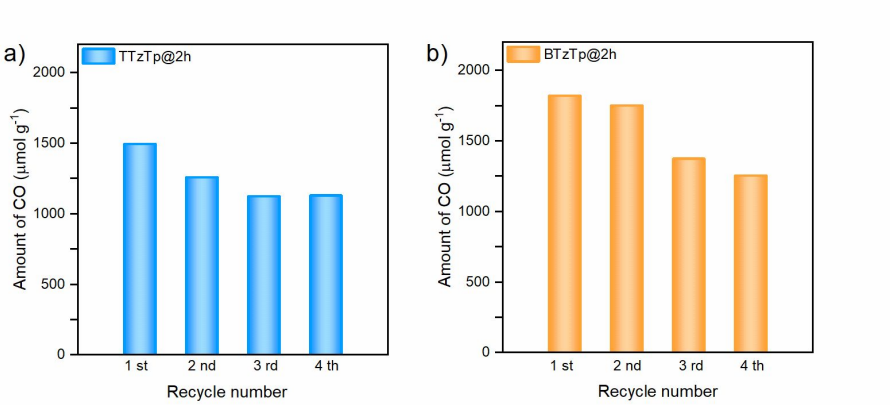


**Figure S10**. Photocatalytic $CO_2$ reduction recyclability test for four times for 2 h production amount respectively (a) TTzTp and (b) BTzTp.

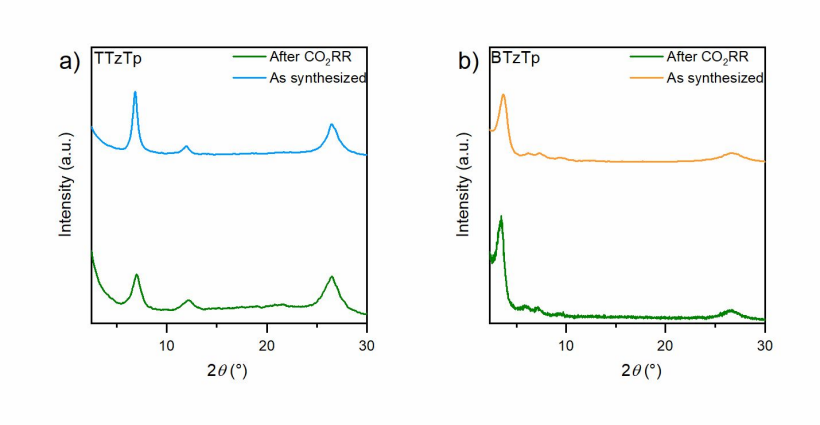


**Figure S11**. PXRD results, as-synthesized (blue and orange line for TTzTp and BTzTp) and after using the COFs (green line), respectively (a) TTzTp and (b) BTzTp.

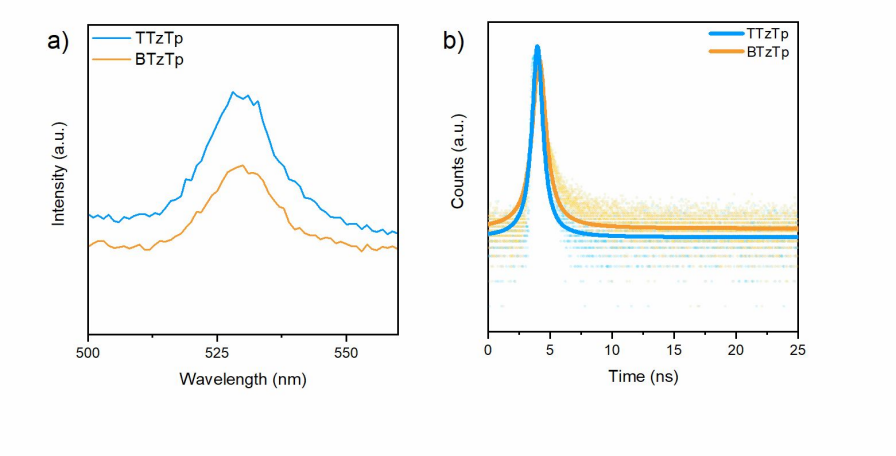


**Figure S12.** (a) Photoluminescence (PL) spectra and (b) lifetime decay curves for TTzTp and BTzTp.

## S9. NMR spectra

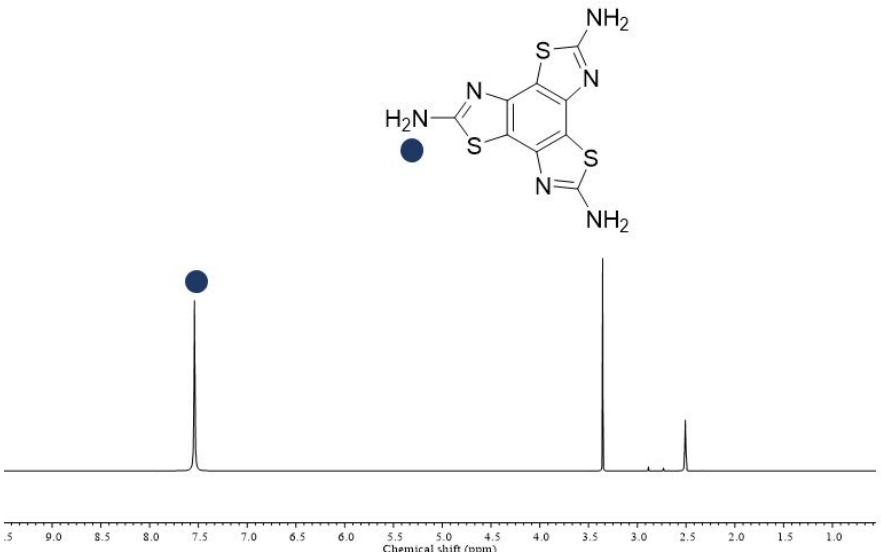


**Figure S13.** Proton NMR spectra of benzo[1,2-d:3,4-d':5,6-d"]tris(thiazole)-2,5,8-triamine (TTz).

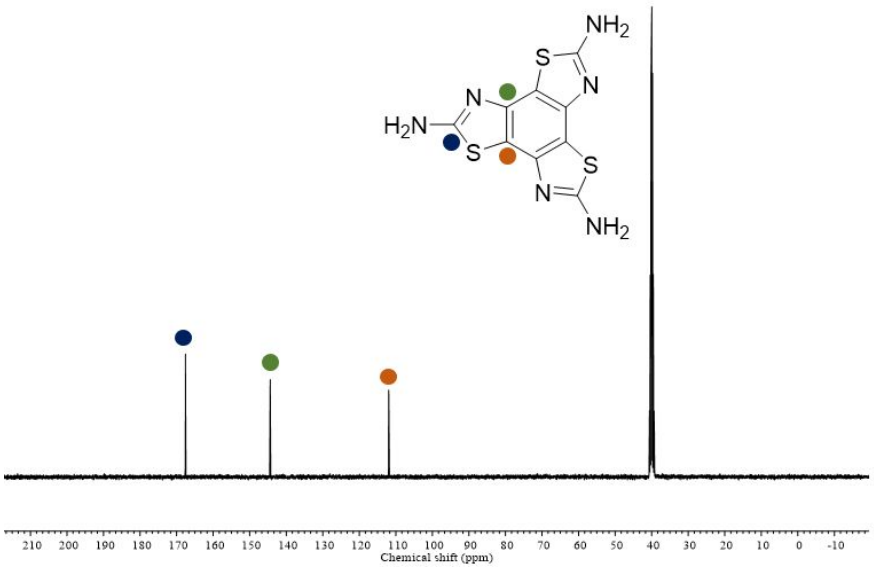


**Figure S14.** Carbon NMR spectra of benzo[1,2-d:3,4-d':5,6-d"]tris(thiazole)-2,5,8-triamine (TTz).